# Power Allocation and Waveform Design for the Compressive Sensing Based MIMO Radar

**YAO YU**
**SHUNQIAO SUN**
Rutgers, The State University of New Jersey

**RABINDER N. MADAN,** Life Fellow, IEEE
Champana Scientific, LLC

**ATHINA PETROPULU,** Fellow, IEEE
Rutgers, The State University of New Jersey

**By exploring sparsity in the target space, compressive sensing (CS) based multi-input multi-output (MIMO) radar systems achieve either the same localization performance as traditional methods but with significantly fewer measurements, or significantly improved performance with the same number of measurements. The work presented here investigates the performance gain of CS-MIMO radars, stemming from optimal power allocation among the transmit antennas, or optimal waveform design. In both cases, the optimization criterion is the minimization of the coherence between the target returns from different search cells, or equivalently, the coherence of the columns of the sensing matrix.**

Manuscript received February 12, 2013; revised October 21, 2013, January 8, 2014; released for publication January 8, 2014.

DOI. No. 10.1109/TAES.2014.130088.

Refereeing of this contribution was handled by M. Weiss.

This work was supported by the Office of Naval Research under Grant ONR-N-00014-12-1-0036.

Authors' addresses: Y. Yu, S. Sun, A. Petropulu, Dept. of Electrical and Computer Engineering, Rutgers, the State University of New Jersey, 94 Brett Road, Piscataway, NJ 08854. E-mail: (athinap@rutgers.edu). R. N. Madan, George Washington University, Washington, D. C.



## I. INTRODUCTION

Due to their potential to improve target detection, multiple-input and multiple-output (MIMO) radar systems have received considerable attention in recent years. Unlike traditional phased-array radar, a MIMO radar transmits multiple independent waveforms from its antennas. Depending on the transmit (TX) and receive (RX) antenna configuration, MIMO radar systems are classified as widely separated [1] and colocated [2]. The former view the target from multiple uncorrelated directions and thus achieve improved target detection performance benefiting from spatial diversity. The latter exploit waveform diversity to form a long virtual array, much longer than traditional radar systems with the same number of TX and RX antennas, and as a result enjoy superior spatial resolution.

Compressive sensing (CS) is a relatively recent development for finding sparse solutions to underdetermined linear systems [3, 4]. CS theory states that a $K$-sparse signal $\mathbf{x}$ of length $N$ can be recovered exactly with high probability from $\mathcal{O}(K \log N)$ linearly compressed measurements. The recovery requires that the product of the measurement matrix and the sparsifying basis matrix, referred to as the sensing matrix, satisfies the uniform uncertainty principle (UUP) [4–6]; in other words, the sensing matrix exhibits low correlation between its columns.

CS in the context of MIMO radars has been studied in [7–12]; [7–9] considered the application of CS to colocated MIMO radars with point targets, while [10–12] considered the application of CS to widely separated MIMO radars with extended targets. Both cases of CS-MIMO radars exploit the sparsity of targets in the target space and enable target estimation based on a small number of samples obtained at the RX antennas.

There are several techniques to further improve the detection performance of CS-MIMO radars. For example, significant gain in range resolution can be achieved by using a step-frequency approach during transmission [13–15]. We can also improve the detection performance by using a measurement matrix that minimizes the coherence of the sensing matrix and/or the signal-to-inference ratio (SIR) [16]. In this paper, we investigate power allocation and/or waveform optimization as a means of improving the detection performance. Previous works [17–19] have discussed power allocation for traditional MIMO radar. In [18], the authors proposed to minimize the total transmitted power such that a predefined Cramer-Rao bound (CRB) is met, or to minimize the CRB by optimizing power allocation among the transmit radars for a given total power budget. A power allocation scheme was proposed in [19] for correlated MIMO radars in the presence of Rician scattering. According to [9], less power is allocated to the antennas that are correlated, or that suffer low line-of-sight reflectivity, so that the total available power is spread across uncorrelated branches and strong reflectors. In [11],

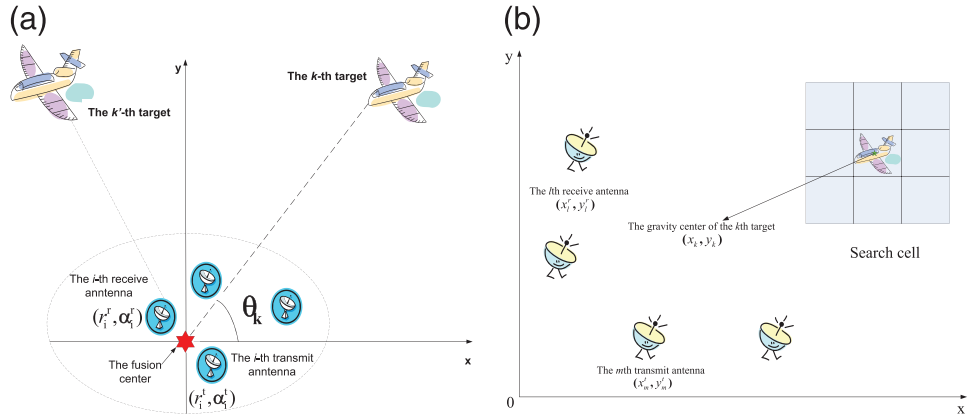


Fig. 1. Two configurations of MIMO radar. (a) colocated case (b) widely separated case.

an energy allocation scheme for widely separated CS-MIMO radars was proposed that determines the transmit energies for the next set of transmit pulses based on the estimates of targets obtained from the previously received signals. The goal of [11] is to maximize the minimum target returns so that the probability of missing weak targets is reduced. In this paper, since UUP indicates that the sensing matrix should be as orthogonal as possible in order to guarantee reliable performance, we allocate the power among the TX antennas so that we minimize the difference between the Gramian of the sensing matrix, i.e., $\mathbf{\Theta}^H \mathbf{\Theta}$ and an identity matrix. Based on the same optimization criterion, we also propose waveform design, aiming at improving the orthogonality of the sensing matrix.

The paper is organized as follows. Section II provides the necessary background and notation for CS-MIMO radars. Section III contains the main results on optimal power allocation and waveform design for collocated CS-based MIMO radars, while Section IV contains the results on optimal power allocation for widely separated CS-MIMO radars. Section V provides simulations to illustrate the theoretical findings, and Section VI contains concluding remarks.

*Notation*: Lower case and capital letters in bold denote, respectively, vectors and matrices. Superscripts $(\cdot)^H$ and $(\cdot)^T$ denote, respectively, the Hermitian transpose and transpose. $\mathbf{0}_{L\times M}$ and $\mathbf{1}_{L\times M}$, respectively, denote an $L \times M$ matrix with "0" and "1" entries. $\mathbf{I}_M$ represents an identity matrix of size $M$. $\otimes$ denotes the Kronecker tensor product.

## II. CS-BASED MIMO RADAR

Let us consider a MIMO radar system consisting of $M_t$ TX antennas and $N_r$ RX antennas. In the far field of the antennas there are $K$ targets that need to be estimated. For simplicity, we assume that the targets are not moving, thus the only parameters that need to be estimated are the target azimuth angles $\theta_k$, $k = 1, \ldots, K$; the results can be easily extended to the case of moving targets. The TX antennas transmit narrowband waveforms, $x_i(t), = 1, \ldots, \mathrm{M}_t$. The RX antennas obtain sub-Nyquist samples of the target returns, and subsequently transmit those samples to a fusion center, where the target estimation is carried out. In the following, we consider separately the cases of colocated and widely separated antennas (as seen in Fig. 1).

### A. Colocated CS-MIMO Radar

Let us assume that the TX and RX antennas are closely spaced and randomly distributed over a small area (see Fig. 1(a)), with the $i$-th TX/RX antenna placed at location $(r_i^t, \alpha_i^t)/(r_i^r, \alpha_i^r)$ (in polar coordinates). Let $L$ denote the number of $T_s$-spaced samples of the transmitted waveforms. At the $l$-th receiver, the received signal is linearly compressed via the measurement matrix $\mathbf{\Phi}$. The effect of the $l$-th compressive receiver [9 (as shown in Fig. 2.) is equivalent to premultiplying a $T_s$-sampled version of the received signal $z_l(t)$ by the $l$-th row of the matrix $\mathbf{\Phi}$. The size of $\mathbf{\Phi}$ is $M \times L$.

Under the far-field and narrowband waveform assumptions and assuming that all the targets are located in the same range cell, the received baseband signal at the $l$-th receive antenna can be approximated by

$$\mathbf{r}_l \approx \sum_{k=1}^{K} \beta_k e^{j\frac{2\pi f}{c}\eta_l^r(\theta_k)} \mathbf{\Phi}\mathbf{X}\mathbf{v}_t(\theta_k) + \mathbf{\Phi}\mathbf{n}_l, \tag{1}$$

where $\mathbf{X}$ is an $L \times M_t$ matrix that contains the transmit waveforms as its columns; $\beta_k$ is the reflection coefficient of the $k$-th target; $\mathbf{v}_t(\theta_k) = [e^{j\frac{2\pi f}{c}\eta_1^t(\theta_k)}, \ldots, e^{j\frac{2\pi f}{c}\eta_{M_t}^t(\theta_k)}]^T$ is the transmit steering vector associated with angle $\theta_k$; $\eta_i^{t/r}(\theta_k) = r_i^{t/r}\cos(\theta_k - \alpha_i^{t/r})$; and $\mathbf{n}_l$ is the interference at the $l$-th receiver, arising due to the interference and thermal noise.

Let us discretize the angle space into $N$ discrete angles $[a_1, \ldots, a_N]$. We assume that the discretization step is small enough so that each target falls on some angle grid point. Then, (1) can be rewritten as

$$\mathbf{r}_l = \underbrace{\mathbf{\Phi}\mathbf{\Psi}_l}_{\mathbf{\Theta}_l}\mathbf{s} + \mathbf{\Phi}\mathbf{n}_l, \tag{2}$$

where $\Psi_l = \left[e^{j\frac{2\pi f}{c}\eta_l^r(a_1)}\mathbf{X}\mathbf{v}_t(a_1), \ldots, e^{j\frac{2\pi f}{c}\eta_l^r(a_N)}\mathbf{X}\mathbf{v}_t(a_N)\right]$; $\mathbf{s} = [s_1, \ldots, s_N]^T$, with $s_n$ being zero if there is no target at angle $a_n$, otherwise being equal to the reflection coefficient of the target at that angle.

By stacking the received data from each antenna into a long vector, we form $\mathbf{y}$, for which it holds

$$\mathbf{y} = \left[\mathbf{r}_1^T, \ldots, \mathbf{r}_{N_r}^T\right]^T = \underbrace{\left[(\mathbf{\Phi}\mathbf{\Psi}_1)^T, \ldots, \left(\mathbf{\Phi}\mathbf{\Psi}_{N_r}\right)^T\right]^T}_{\mathbf{\Theta}}\mathbf{s} + \underbrace{\left[(\mathbf{\Phi}\mathbf{n}_1)^T, \ldots, \left(\mathbf{\Phi}\mathbf{n}_{N_r}\right)^T\right]^T}_{\mathbf{z}}. \quad (3)$$

If the number of targets is small as compared with $N$, then $s$ is a sparse vector, with the locations of its non-zero elements providing information on the target angles. A variety of CS methods can be applied to the recovery of s, e.g., basis pursuit [20], matching pursuit [21] and Lasso methods [22]. According to the CS formulation, $\mathbf{\Theta}$ is the sensing matrix and $\mathbf{\Psi}_l$ is the basis matrix for the $l$-th antenna.

### B. Widely Separated CS-MIMO Radar

We consider an antenna configuration with multiple TX and RX antennas that are arbitrary located over a large area (see Fig. 1(b)). We assume that there are $K$ extended targets in the search space, each one consisting of $Q$ independent, isotropic scatterers. For simplicity, the targets and the antennas are taken to be on the same plane and the targets are stationary. Let $(x_i^t, y_i^t)$ and $(x_i^r, y_i^r)$ denote the locations of the $i$-th TX and RX antenna, respectively, and let $(x_{qk}, y_{qk})$ denote the location of the $q$-th scatterer of the $k$-th target at the initial time of sampling. All locations in this section are given in Cartesian coordinates. The distance between the $i$-th TX/RX antenna and the $q$-th scatterer of the $k$-th target at time $t$ equals:

$$d_{qki}^{t/r}(t) = \sqrt{\left(x_{qk} - x_i^{t/r}\right)^2 + \left(y_{qk} - y_i^{t/r}\right)^2} \quad (4)$$

For stationary targets, the parameters to be estimated are $x_{qk}, y_{qk}$, $\mathrm{q} = 1, \ldots, \mathrm{Q}$, $k = 1, \ldots, K$. The baseband signal due to the $i$-th transmit antenna arrives at the $l$-th receive antenna as [1]

$$z_{il}(t) = \sum_{k=1}^{K}\sum_{q=1}^{Q} h_{qk}^{il} x_i\left(t - \frac{d_{qki}^t(t) + d_{qkl}^r(t)}{c}\right) + n_{il}(t), \quad l = 1, \ldots, M_r \quad (5)$$

where $h_{qk}^{il}$ is the attenuation coefficient associated with the $q$-th scatterer of the $k$-th target and the TX/RX antenna pair $(i, l)$, and $n_{il}(t)$ denotes interference. Assuming that the antennas transmit on different channels, or at different times, the target returns due to each transmit antenna can be separated.

With sufficiently narrowbanded TX waveforms, the target scatterers are unresolvable, and thus each extended target can be represented by its center of gravity $(x_k, y_k)$. Therefore, $x_i(t - \frac{d_{qki}^t(t)+d_{qkl}^r(t)}{c}) \approx x_i(t - \frac{d_{ki}^t(t)+d_{kl}^r(t)}{c})$, where $d_{ik}^t = \sqrt{(x_i^t - x_k)^2 + (y_i^t - y_k)^2}$. Thus, (5) can be approximated as [1]

$$z_{il}(t) \approx \sum_{k=1}^{K} h_k^{il} x_i(t - \tau_{ik} - \tau_{kl}) + n_{il}(t), \quad (6)$$

where $\tau_{ik} = d_{ik}^t/c$ is the propagation delay between the $i$-th transmit antenna and the gravity center of the $k$-th target; $\tau_{kl}$ is the propagation delay between the gravity center of the $k$-th target and the $l$-th receive antenna; $h_k^{il} = \sum_{q=1}^{Q} h_{qk}^{il}$ represents the channel gain associated with the $k$-th target and the TX-RX antenna pair $(i, l)$.

Let us discretize the target space into $N$ grid points, i.e., $[(x_n, y_n)]$, $n = 1, \ldots, N$ and let $s_n^{il}$ denote the coefficient associated with the $n$-th grid point for the TX-RX antenna pair $(i, l)$. Equation (6) can be rewritten as a linear combination of target returns reflected from all grid points, i.e.,

$$r_{il}(t) = \sum_{n=1}^{N} s_n^{il} x_i(t - \tau_{in} - \tau_{nl}) + n_{il}(t) = \mathbf{p}_{il}^T(t)\,\mathbf{s}^{il} + n_{il}(t), \quad (7)$$

where $\mathbf{p}_{il}(t) = [x_i(t - \tau_{i1} - \tau_{1l}), \ldots, x_i(t - \tau_{iN} - \tau_{Nl})]^T$ and $\mathbf{s}^{il} = [s_1^{il}, \ldots, s_N^{il}]^T$. If there is a target at $(x_n, y_n)$, the coefficient $s_n^{il}$ equals the channel gain associated with the corresponding target and the antenna pair $(i, l)$; otherwise, $s_n^{il}$ equals zero.

In vector form, the compressed measurements received at the $l$-th receive antenna can be expressed as

$$\mathbf{y}_{il} = \mathbf{\Phi}\left[r_{il}(0T_s), \ldots, r_{il}((L-1)T_s)\right]^T = \underbrace{\mathbf{\Phi}\mathbf{\Psi}_{il}}_{\mathbf{\Theta}_{il}}\mathbf{s}^{il} + \mathbf{\Phi}\mathbf{n}_{il}, \quad (8)$$

where $\mathbf{\Psi}_{il} = [\mathbf{p}_{il}(0T_s), \ldots, \mathbf{p}_{il}((L-1)T_s)]^T$, $\mathbf{n}_{il} = [\mathrm{n}_{il}(0T_s), \ldots, n_{il}((L-1)T_s)]^T$, and $\mathbf{\Phi}$ is the measurement matrix that is used to compress the received data and is defined in Section II-A.

The samples from all receive antennas are sent to a fusion center, which formulates a vector $\mathbf{y}$ of length $M_t N_r L$, i.e.,

$$\mathbf{y} = \left[\mathbf{y}_{11}^T, \ldots, \mathbf{y}_{1N_r}^T, \mathbf{y}_{M_t1}^T, \ldots, \mathbf{y}_{M_tN_r}^T\right]^T = diag\left\{\left[\mathbf{\Theta}_{11}, \mathbf{\Theta}_{12}, \ldots, \mathbf{\Theta}_{M_tN_r}\right]\right\}\mathbf{s} + \mathbf{n}, \quad (9)$$

where $\mathbf{s} = \left[\left(\mathbf{s}^{11}\right)^T, \left(\mathbf{s}^{12}\right)^T, \ldots, \left(\mathbf{s}^{M_tN_r}\right)^T\right]^T$ and $\mathbf{n} = \left[(\mathbf{\Phi}\mathbf{n}_{11})^T, (\mathbf{\Phi}\mathbf{n}_{12})^T, \ldots, (\mathbf{\Phi}\mathbf{n}_{M_tN_r})^T\right]^T$. Note that for all pairs $(i, l)$, the vector $\mathbf{s}^{il}$ contains mostly zeros except at locations corresponding to grid points occupied by targets. Thus, $\mathbf{s}$ is a sparse vector. If there is a target at the $n$-th grid point, all $n$-th entries of $\mathbf{s}^{il}$ corresponding to all TX-RX antenna pairs, i.e., $s_n^{il}$, $i = 1, \ldots, M_t$, $l = 1, \ldots, N_r$, are non-zero. Therefore, by appropriately rearranging the columns of the basis matrix, the non-zero elements of $\mathbf{s}$ corresponding to different pairs and the same target can be clustered together, thus making $\mathbf{s}$ appear as

group sparse. On letting $\mathbf{u}_{il}^n$ denote the $n$-th column of $\mathbf{\Theta}_{il}$, the columns of the basis matrix $\mathbf{\Psi}_g$ that induces group sparsity can be arranged as follows [12, 11]:

$$\mathbf{\Psi}_g = \left[\widetilde{\mathbf{\Psi}}_1, \ldots, \widetilde{\mathbf{\Psi}}_N\right] \tag{10}$$

where $\widetilde{\mathbf{\Psi}}_n = diag\left\{\left[\mathbf{u}_{11}^n, \ldots, \mathbf{u}_{1N_r}^n, \mathbf{u}_{21}^n, \ldots, \mathbf{u}_{M_tN_r}^n\right]\right\}$.

The sparse vector $\mathbf{s}$ associated with $\mathbf{\Psi}_g$ contains $K$ groups of non-zeros entries and each group is of length $M_tN_r$. When recovering $\mathbf{s}$, its group sparsity can be exploited using the group Lasso approach [23, 24], i.e.,

$$\arg\min_{\mathbf{s}} \underbrace{\frac{1}{2}||(\mathbf{y} - \Psi_g\mathbf{s})||_2^2}_{f_1(\mathbf{s})} + \underbrace{\lambda \sum_{n=1}^{N} ||\mathbf{s}_n||_2}_{f_2(\mathbf{s})} \tag{11}$$

where $\mathbf{s}_n = [s_n^{11}, \ldots, s_n^{M_tN_r}]$. $f_2(\mathbf{s})$ can be recast as the $l_1$ norm of the vector $\lambda[||\mathbf{s}_1||_2, \ldots, ||\mathbf{s}_N||_2]^T$. Minimization of $f_2(\mathbf{s})$ produces a group-sparse solution [23, 24]. Due to the nature of the $l_2$ norm, all entries of the $n$-th group $\mathbf{s}_n$ will be zero if $||\mathbf{s}_n||_2$ is zero, and will be non-zero otherwise. Since $f_2(s)$ is nonsmooth, it is not trivial to directly
solve (11). Instead of minimizing $f_1(s)$ and $f_2(s)$ simultaneously, the proximal gradient algorithm [25–27] proceeds by dealing with $f_1(s)$ and $f_2(s)$ individually in an iterative way. Let $\hat{\mathbf{s}}$ denote the solution to (11). We can formulate the target indicator vector $\mathbf{d}$ so that its $n$-th entry equals $||\hat{s}_n||_2^2$. The peaks of $\mathbf{d}$ will provide the target information.

## III. POWER ALLOCATION AND WAVEFORM DESIGN FOR COLOCATED CS-BASED MIMO RADAR

### A. Power Allocation

It should be noted that the proposed power allocation (PPA) scheme aims at direction of arrival (DOA) estimation only, since under the stated assumptions the range information is absorbed by the target reflection coefficients $\beta_k, k = 1, \ldots, K$ and thus cannot be identified based on the model of (1). In the general case, in which, the targets are located in different range cells, a range dependent time delay would be introduced in the waveforms [13]. In that case a discretization of the range-DOA space would be required in order to construct the basis matrix (see [13]). However, unless the bandwidth of the transmitted signal is increased, the above-described MIMO radar approach cannot improve range estimation as compared with single-input single-output (SISO) radars. Approaches to improve range resolution in the context of CS MIMO radar, such as using step-frequency ideas, have been discussed in [13]. In the following, we focus on DOA estimation only.

UUP [4–6] indicates that the sparse vector can be recovered with high probability if the sensing matrix is orthogonal. This is impossible for a fat measurement matrix, however, we can force the sensing matrix before and after $\mathbf{\Theta}$ to be as orthogonal as possible, i.e., by minimizing the difference between $\mathbf{\Theta}^H\,\mathbf{\Theta}$ and an identity matrix of size $N$. Let $\mathbf{p} = [p_1, \ldots, p_{Mt}]^T$ denote the transmit power allocated to $M_t$ TX antennas, with $\sum_{i=1}^{M_t} p_i = P_t$. Then, the $k$-th column of the sensing matrix equals

$$\mathbf{u}_k = \left[e^{j2\pi\frac{\eta_1^r(a_k)f}{c}}, \ldots, e^{j2\pi\frac{\eta_{N_r}^r(a_k)f}{c}}\right]^T \otimes (\Phi\mathbf{X}\mathbf{V}(a_k)\hat{\mathbf{p}}) \tag{12}$$

where $\mathbf{V}(a_k) = \text{diag}\{\mathbf{v}_t(a_k)\}$ and $\hat{\mathbf{p}} = \sqrt{\mathbf{p}}$. Suppose that the MIMO radar system has a fixed total power budget for transmission, equal to $P_t$. We next determine how $P_t$ should be distributed among the transmit antennas so that it results in improved CS recovery performance.

The power allocation problem can be formulated as follows:

$$\begin{aligned} &\min_{\tilde{\mathbf{p}}} \sum_{k\neq k'} |\mathbf{u}_{k'}^H\mathbf{u}_k|^2 + \sum_k |\mathbf{u}_k^H\mathbf{u}_k - P_tN_r|^2 \\ &s.t.\ \tilde{\mathbf{p}}^T\tilde{\mathbf{p}} = P_t,\ \tilde{\mathbf{p}} \geq \mathbf{0}_{M_t\times 1},\ \tilde{\mathbf{p}} \leq \sqrt{P_m}\mathbf{1}_{M_t\times 1} \end{aligned} \tag{13}$$

where the objective function is the squared difference between $\mathbf{\Theta}^H\,\mathbf{\Theta}$ and $P_tN_r\mathbf{I}_N$, with the first term, denoted by SCSM, being the sum of the square magnitude of the cross-correlation of column pairs $\mathbf{u}_k, \mathbf{u}_{k'}$ of the sensing matrix. $P_m$ is the maximum transmit power of each TX antenna. The objective function can be transformed into a convex function but the constraints are not convex. The details of the algorithm, which solves the optimization problem of (13), are given in the Appendix.

One could use a compressive receiver at each receive antenna, based on some measurement matrix $\mathbf{\Phi}$. However, the implementation of the measurement matrix may increase the complexity of the analog circuit. Therefore, we can skip the step of linear compression and directly collect a small number of sub-Nyquist samples at the RX antennas. If the TX antennas transmit orthogonal waveforms, i.e., $\mathbf{X}^H\mathbf{X} = \mathbf{I}$, then $\mathbf{B}_{kk}$ is a diagonal matrix. Then (13) can be reduced to a simple convex problem as follows:

$$\begin{aligned} &\min_{\mathbf{p}}\ \mathbf{p}^T\left(\sum_{k\neq k'} u_{kk'}\mathbf{b}_{kk'}^*\mathbf{b}_{kk'}^T\right)\mathbf{p} \\ &s.t.\mathbf{1}_{M_t\times 1}^T\mathbf{p} = P_t,\ \mathbf{p} \geq \mathbf{0},\ \mathbf{p} \leq P_m\mathbf{1}_{M_t\times 1} \end{aligned} \tag{14}$$

where $\mathbf{b}_{kk'}$ is the diagonal vector of $\mathbf{B}_{kk'}$.

We should note here that the power allocation vector obtained from (13) or (14) does not affect the SIR since the total transmitted power is fixed. Therefore, the performance gain stems from the improved sensing matrix only. If some TX antennas contribute to the sensing matrix negatively, the power allocated to them will be very small. This indicates that the proposed scheme will effectively reduce the number of active TX antennas as compared to a scheme that uses uniform power allocation (UPA) across all antennas.

### B. Waveform Design

Along the lines of optimal power allocation, we can also optimize the transmit waveforms to further improve

the performance of the CS-based MIMO radars. Let us again consider as design criterion the minimization of the difference between the Gramian of the sensing matrix and an identity matrix for a fixed total transmit power. The $k$-th column of the sensing matrix becomes

$$\mathbf{u}_k = \left[ e^{j2\pi \frac{\eta_1^r(a_k)f}{c}}, \ldots, e^{j2\pi \frac{\eta_{N_r}^r(a_k)f}{c}} \right]^T \otimes (\mathbf{\Phi}\widetilde{\mathbf{V}}(a_k)\mathbf{x}) \tag{15}$$

where $\widetilde{\mathrm{V}}(a_k) = \mathbf{I}_L \otimes \mathbf{v}_t^T(a_k)$ and $\mathbf{x} = vec(\mathbf{X}^T)$. Since the total power is set to $P_t$, it holds that $\mathbf{x}^H\mathbf{x} = P_t$.

We can formulate the following optimization problem:

$$\begin{aligned} &\min_{\mathrm{x}} \sum_{k\neq k'} |\mathbf{u}_{k'}^H\mathbf{u}_k|^2 + \sum_k |\mathbf{u}_k^H\mathbf{u}_k - P_tN_r|^2 \\ &s.t.\ \mathbf{x}^H\mathbf{x} = P_t \end{aligned} \tag{16}$$

The optimization problem above almost takes the same form as (13) and so we can follow the procedure described in the Appendix to solve this problem. The following points are worth noting.

1) Equation (16) is not convex and thus we can only find a local minimum, which depends on the initial waveforms. Still, as shown in the simulations section, this approach can lead to performance improvement.

2) For simplicity, the objective function in (16) is formulated as a function of DOA only. In the general case, where the targets are located in different range cells and are moving, a target/range dependent time delay will be introduced in the waveforms, and a Doppler shift will appear in the phase term [13]. Such model would require searching for targets in a three-dimensional (3-D) space, i.e., range-DOA-speed space, and thus the basis matrix would need to be formulated based on a grid in this 3-D space (more details about joint range-DOA-speed estimation and its reduced complexity implementation can be found in [13]). The proposed method in this work can be straightforwardly extended to the aforementioned model involving range, DOA, and speed. In that case, the solution to (16) would enable improved range and Doppler estimation as well as DOA estimation.

3) The procedure of the Appendix can be used to solve both power allocation (13) and waveform design (16). However, the number of variables for waveform design is much larger than that for power allocation, i.e., the former is $M_tL$ while the latter is $M_t$.

## IV. POWER ALLOCATION FOR WIDELY SEPARATED CS-BASED MIMO RADAR

Suppose that the total power is set to $P_t$. Let $\mathbf{p}$ denote the transmit power allocated to $M_t$ TX antennas, and thus $\sum_{i=1}^{M_t} p_i = P_t$. Again, we force $\mathbf{\Phi}_g$ to be as orthogonal as possible by minimizing the difference between the Gramian matrix of the sensing matrix, i.e., $\mathbf{\Phi}_g^H\mathbf{\Phi}_g$, and an identity matrix of size $M_tN_rN$. In particular, we formulate the following optimization problem:

$$\begin{aligned} &\min_{\mathbf{p}} \ ||\mathbf{\Phi}_g^H\mathbf{\Phi}_g - \mathbf{I}||_F^2 \\ &s.t.\ \mathbf{1}_{M_t\times 1}^T\mathbf{p} = P_t,\ \mathbf{p} \geq \mathbf{0}_{M_t\times 1},\ \mathbf{p} \leq P_m\mathbf{1}_{M_t\times 1} \end{aligned} \tag{17}$$

where $P_m$ is the maximum transmitted power accepted by a TX antenna.

The Gramian matrix $\mathbf{\Phi}_g^H\mathbf{\Phi}_g$ can be rewritten as

$$\begin{aligned} \mathbf{\Phi}_g^H\mathbf{\Phi}_g &= \left[\widetilde{\mathbf{\Psi}}_1, \ldots, \widetilde{\mathbf{\Psi}}_N\right]^H \left[\widetilde{\mathbf{\Psi}}_1, \ldots, \widetilde{\mathbf{\Psi}}_N\right] \\ &= \begin{bmatrix} \mathbf{D}_p\mathbf{D}_{11} & \cdots & \mathbf{D}_p\mathbf{D}_{1N} \\ \vdots & \ldots & \vdots \\ \mathbf{D}_p\mathbf{D}_{1N} & \cdots & \mathbf{D}_p\mathbf{D}_{NN} \end{bmatrix} \end{aligned} \tag{18}$$

where $\mathbf{D}_{kk'} = \widetilde{\mathbf{\Psi}}_k^H\widetilde{\mathbf{\Psi}}_{k'},\ k,k' = 1,\ldots,N$ are diagonal matrices due to the special sparse structure of $\widetilde{\mathbf{\Psi}}_N$ as shown in (10) and $\mathbf{D}_p = diag\{\mathbf{p}\otimes\mathbf{1}_{N_r\times 1}\}$. Since the waveform of each TX antenna is of unit power, it holds that $\mathbf{D}_{kk} = \mathbf{I},\ k = 1,\ldots,N$.

Let $\mathbf{d}_i^{kk'}$ denote the $i$-th group of the diagonal elements of $\mathbf{D}_{kk'}$, whose length is $N_r$. Then the optimization problem (17) can be further written as

$$\begin{aligned} &\min_{\mathbf{p}} \ \mathbf{p}^T\mathbf{D}\mathbf{p} + N_r\mathbf{p}^T\mathbf{p} \\ &s.t.\ \mathbf{1}_{M_t\times 1}^T\mathbf{p} = P_t,\ \mathbf{p} \geq \mathbf{0}_{M_t\times 1},\ \mathbf{p} \leq P_m\mathbf{1}_{M_t\times 1} \end{aligned} \tag{19}$$

where $\mathbf{D}$ is a diagonal matrix whose $i$-th diagonal element equals $\sum_{k\neq k'} |\mathbf{d}_i^{kk'}|_2^2$. The first term of the objective function sums up the squared correlation of cross column pairs in the sensing matrix. The second term represents the squared error between the column norm of the sensing matrix and 1, in which the constant terms have been removed.

One may wonder whether minimizing (19) requires that the column norms of the sensing matrix approach 1, or equivalently, $\mathbf{p}$ approaches a unit vector. For large $N$, the second term in the objective function is small as compared with the first term, so that the solution $\mathbf{p} = \mathbf{1}$ can be avoided. From the perspective of the CS recovery methods, the column norm of the sensing matrix for the group Lasso method is not as important as in the Lasso method, since the group Lasso approach forces the coefficients within a group to be non-zero or zero simultaneously. This indicates that the sum of the squared norm of the columns within a group (SSNCG), rather than of a single column of the sensing matrix, weighs in the group Lasso approach. Due to the special structure of the sensing matrix, as seen in (10), the SSNCG of different groups is the same, independent of the power vector $\mathbf{p}$, and lies between $\frac{P_t^2}{M_t}$ and $CP_m^2 + (P_t - CP_m)^2$, where $C = \lfloor P_t/P_m \rfloor$. Therefore, the column norm of the sensing matrix does not have to approach 1 when the group Lasso method is used. It is also reasonable to remove $\mathbf{p}^T\mathbf{p}$ from the objective function.

The power allocation vector obtained from (19) will not affect the SIR since the total transmit power is fixed.

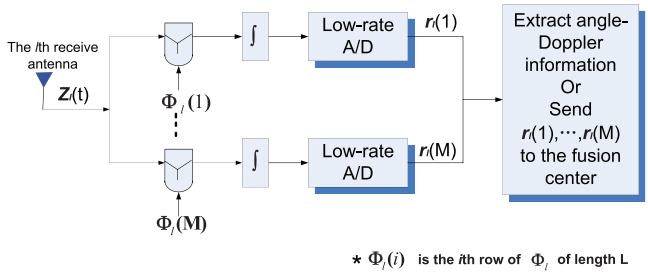


Fig. 2. Fig. 1 of [9].

Therefore, the performance gain stems from the improved sensing matrix only. If some TX antennas contribute to the sensing matrix negatively, the power allocated to those TX antennas would be reduced. In the case of colocated MIMO radar where the TX antennas view the target from the same angle, each RX antenna receives a superposition of delayed versions of all transmit waveforms. In other words, the columns of basis matrix are the weighted sum of the waveforms from multiple TX antennas. This model induces TX antenna redundancy. Unlike colocated MIMO radar, all TX antennas are needed for widely separated MIMO radar. This is because the antennas in this case see different aspects of the target and so the received signals due to each TX-RX antenna are separated and stacked together at the fusion center.

## V. SIMULATIONS

### A. Power Allocation and Waveform Design for Colocated CS-Based MIMO Radar

1) *Power Allocation*: We consider a MIMO radar system with the TX and RX antennas, uniformly located on a disk of radius 10 m, as shown in Fig. 1(a). The carrier frequency is $f = 5$ GHz. The transmitted waveforms are orthogonal Hadamard sequences with $L = 32$ and have unit power. At each receive antenna, the received signal is corrupted by zero-mean Gaussian noise of power $\sigma^2$. The signal-to-noise ratio (SNR) is defined as $1/\sigma^2$. Three targets are present on the angle grid $[0^\circ, 0.1^\circ, \ldots, 5^\circ]$. We should note that a small grid was considered here in order to keep the computational complexity low. The total transmitted power is set to $M_t$ and the maximum transmit power for each antenna is 9 W. In the simulations, the identity matrix is used as the measurement matrix $\mathbf{\Phi}$ (Fig. 2). Based on the received compressed measurements in (3), we use the Dantzig selector [28] to recover $\hat{\mathbf{s}}$, which contains the angle information on targets, i.e.,

$$\hat{\mathbf{s}} = \min ||\mathbf{s}||_1 \quad s.t. ||\mathbf{\Theta}^H(\mathbf{y} - \mathbf{\Theta}s)||_\infty < \mu. \qquad (20)$$

In the above, the sensing matrix $\Theta$ is formed by using the optimal power allocation vector, which is obtained by solving the problem of (14) using CVX, a package for specifying and solving convex programs [29].

Multiple independent runs are conducted; in each run the locations of TX and RX antennas are randomly generated following a uniform distribution. Fig. 3 demonstrates the average coherence of column pairs of the sensing matrix, corresponding to the PPA scheme, computed over 100 independent runs and for $M_t = 5,\ 10,\ 15,\ 20,\ 25,\ 30$. For comparison purposes, the corresponding results for UPA and random power allocation (RPA) are also shown in the same figure. It can be seen from the figure that the PPA scheme can reduce the SCSM as compared with the UPA and RPA schemes. Fig. 3 also shows that the SCSM can be reduced by increasing the number of RX antennas.

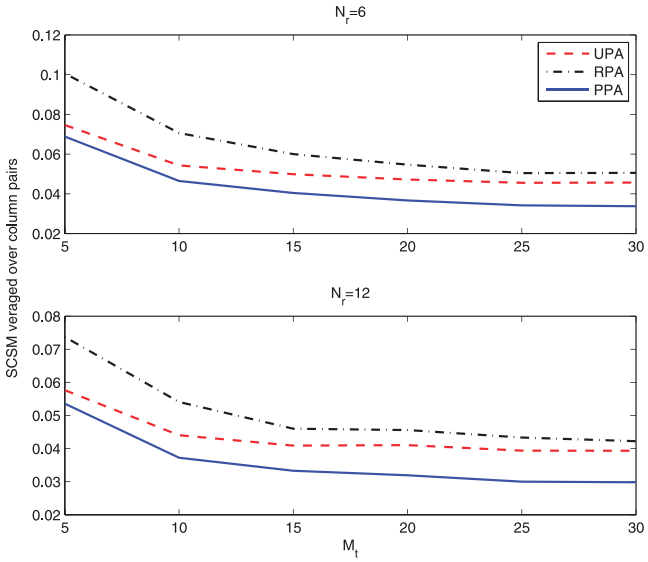


Fig. 3. SCSM versus $M_t$ under optimal power allocation (PPA), UPA, and RPA in CS-based colocated MIMO radars. Case (I) $N_r = 6$; case (II) $N_r = 12$; in both cases $L = 32$.

Fig. 4 shows the receiver operating characteristic (ROC) curves of the angle estimates, obtained based on 1000 independent runs. In each run, three targets are randomly generated on the angle grids. Here, the probability of detection (PD) is the percentage of cases in which all the targets are detected. The probability of false alarm (PFA) is defined as the percentage of cases in which false targets are detected. The cases of SNR = –10 dB, 0 dB with a different number of TX/RX antennas are shown in Fig. 4. One can see that the PPA scheme has improved ROC performance as compared to the UPA scheme. Again, an increase in the number of RX antennas can improve the detection performance. Increasing the number of RX antennas cannot boost SNR and thus the performance gain comes from the improvement of the sensing matrix, as shown in Fig. 3. The performance gain with the increase of the number of TX/RX antennas is more prominent at low SNR. This is because using more TX/RX antennas effectively increases the array aperture. In addition, an increase in the number of TX antennas can also improve the SNR of the received signal at the RX antennas, as in our simulations the transmit power for each TX antenna is fixed.

In addition to performance improvement, the PPA scheme also reduces the number of active TX antennas.

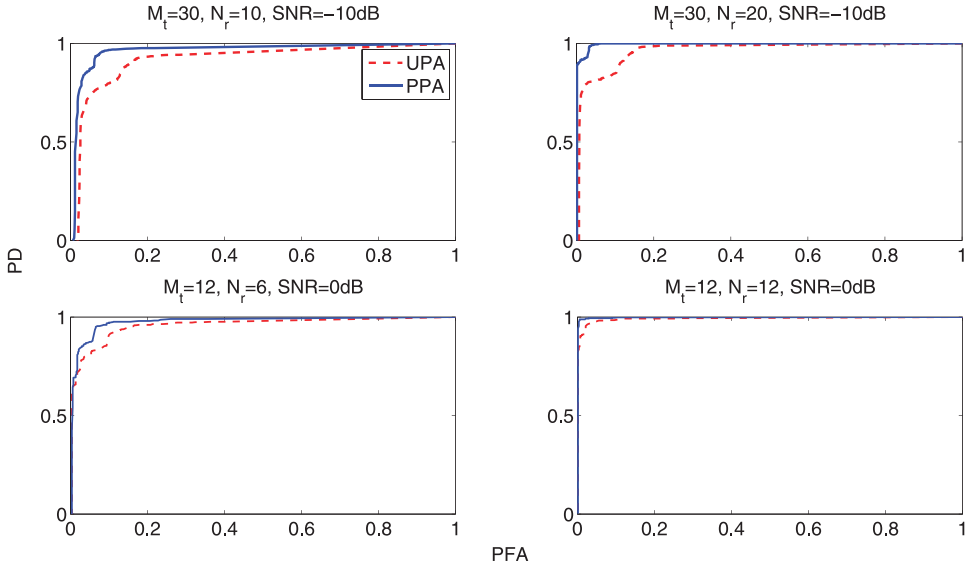


Fig. 4. ROCs of angle estimates under power allocation in CS colocated MIMO radars with $L = 32$.

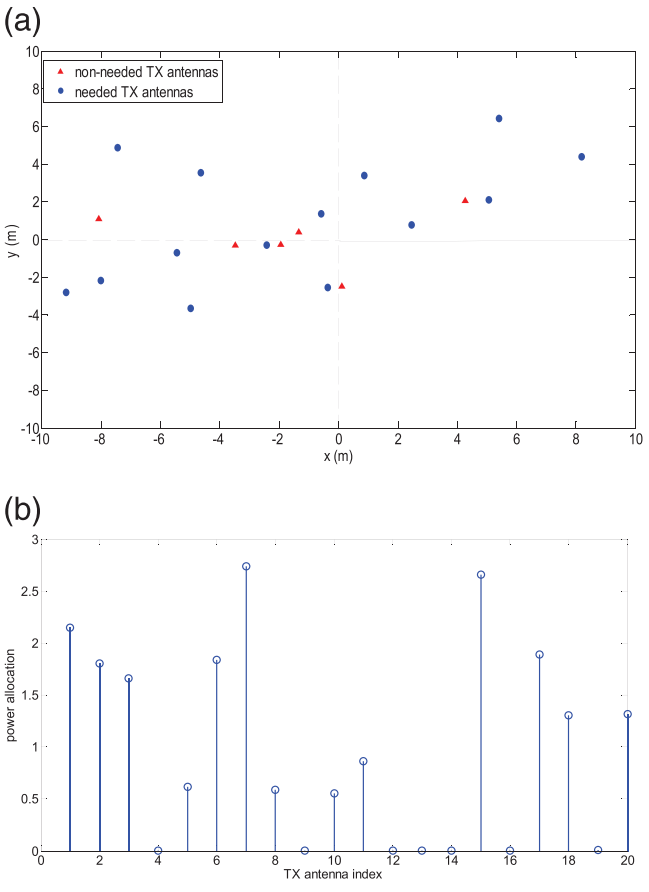


Fig. 5. TX distribution in CS colocated MIMO radars with $M_t = 20$, $N_r = 12$, and $L = 32$. (a) TX antenna distribution. (b) Power allocation.

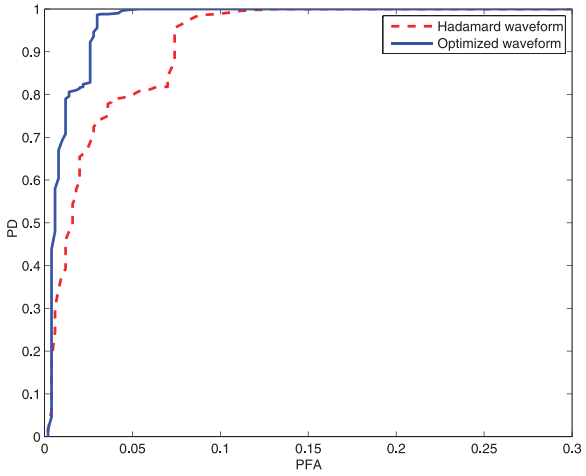


Fig. 6. ROCs of angle estimates under waveform design in CS-based colocated MIMO radars with $M_t = N_r = 10$ and $L = 16$.

For example, on an average, and in 500 runs, in the case of $M_t = 20$ and $N_r = 12$, 6 TX antennas are allocated power less than 0.0001 W. This indicates that the PPA scheme only requires 14 TX antennas to be active, while all 20 TX antennas are needed for the UPA scheme. Fig. 5(a) shows the distribution of TX antennas which were assigned power less than 0.0001 W in one run; the nonneeded antennas are marked on the figure. Fig. 5(b) demonstrates the power allocation results in this case.

2) *Waveform Design*: We consider the same antenna configuration as above. The received signal is corrupted by zero-mean Gaussian noise of unit power. Three targets are present on the angle grid $[0^\circ, 0.2^\circ, \ldots, 2^\circ]$. The total transmitted power is set to $M_t$. The initial waveform $\mathbf{x}^{(0)}$ uses an orthogonal Hadamard sequence of length $L = 16$ and unit power. The measurement matrix $\mathbf{\Phi}$ is chosen as a random matrix with $M = \text{round}\,(0.7L)$, which means that each RX antenna forwards $M = 11$ samples. The ROC curve of the angle estimates produced by the proposed waveform design method is shown in Fig. 6, where the performance improvement due to the designed waveform

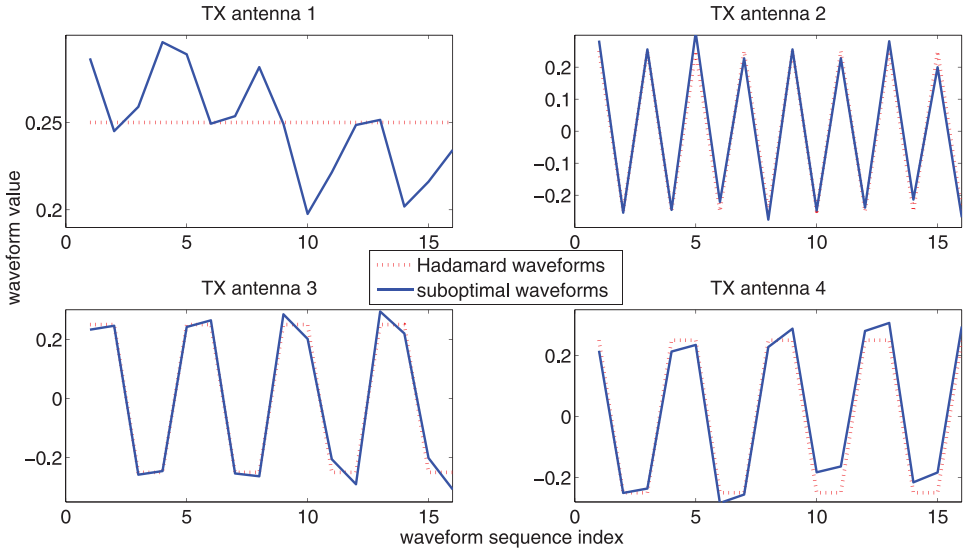


Fig. 7. Local optimum waveforms and initial waveforms of 4 TX antennas in one run for CS-based colocated MIMO radars with $M_t = N_r = 10$ and $L = 16$.

is evident. Fig. 7 illustrates the suboptimal waveforms of 4 TX antennas obtained from (16) in one run.

## B. Power Allocation for Widely Separated CS-Based MIMO Radar

In this section, we demonstrate the performance of the PPA and the UPA schemes based on the group Lasso method in the context of widely separated MIMO radar. We consider a MIMO radar system with TX and RX radars that are uniformly located on a circle of radius 6000 m and 3000 m, respectively. The carrier frequency is $f = 5$ GHz. Each transmit radar uses orthogonal Hadamard waveform sequences of length $L = 20$, and unit power. In the simulations, the measurement matrix $\mathbf{\Phi}$ is chosen as an identity matrix. Three targets are assumed to be present in the search space [1000, 1050, . . . ,1200] m $\times$ [1000, 1050, . . . ,1200] m, and in each run, the targets are randomly located on grid points. The target reflectivity is a Gaussian random variable with unit variance. The total power varies with the number of TX antennas and is set to $M_t$. The power threshold for each TX antenna is 2.

Fig. 8 compares the PPA and the UPA schemes in terms of the squared difference between the Gramian of the sensing matrix and the identity matrix (SEGI), averaged over the $N\ M_t N_r$ elements of the Gramian matrix of the sensing matrix. It can be seen from Fig. 8 that the PPA scheme reduces SEGI as compared with UPA, and also that the SEGI decreases with the number of TX and RX antennas.

Fig. 9 shows the ROC curves of the angle estimates, obtained based on 1000 independent runs. In each run, three targets are randomly generated on the angle grid of interest. Four cases are shown, i.e., ($M_t = 10,\ N_r = 1,$ SNR $= 10$ dB), ($M_t = 5,\ N_r = 2,$ SNR $= 10$ dB),

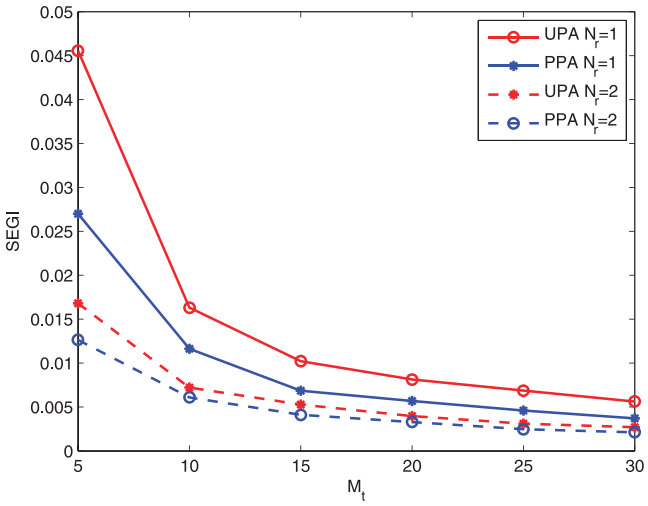


Fig. 8. SEGI versus $M_t$ under optimal and UPA in CS-based widely separated MIMO radar with $L = 20$.

($M_t = 10,\ N_r = 1,$ SNR $= 20$ dB), and ($M_t = 5,\ N_r = 2,$ SNR $= 20$ dB). One can see that the PPA scheme has improved ROC performance as compared to the UPA scheme. With the same number of TX and RX antennas, the performance improvement of the PPA scheme diminishes at higher SNR. Fig. 10 shows the distribution of TX and RX antennas in one run where $M_t = 10$, $N_r = 1$, and power allocation is based on PPA. Unlike in the colocated MIMO radar case, all TX antennas are needed for widely separated MIMO radar. This is because the antennas in this case see different aspects of the target and thus the received signals due to all TX-RX antenna pairs are separated and stacked together at the fusion center.

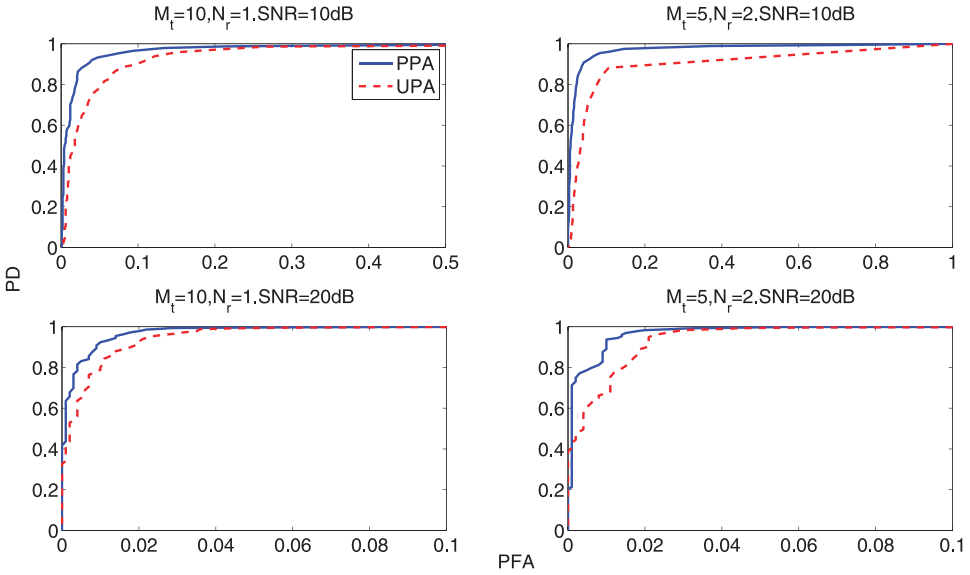


Fig. 9. ROC of target location estimates under power allocation in CS-based widely separated MIMO radars with four combinations of $M_t$ and $N_r$.

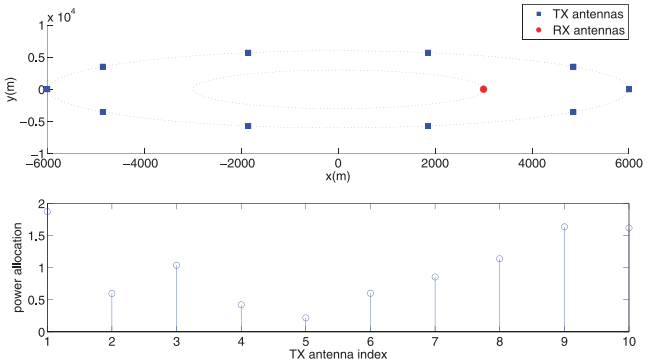


Fig. 10. TX distribution in CS widely separated MIMO radars with $M_t = 10,\ N_r = 1$ and $L = 32$.

## VI. CONCLUSIONS

We have proposed power allocation schemes for colocated and widely separated CS-based MIMO radars. The proposed schemes aim at rendering the sensing matrix as orthogonal as possible. It has been shown that the estimation of DOA can be improved by allocating the available power budget to the TX antennas in an optimal fashion. Such allocation can reduce the number of active TX antennas as compared with the UPA scheme. This is because the TX antennas that cause the sensing matrix to be more correlated are eliminated by the PPA scheme. Along the lines of optimal power allocation, we also developed a waveform design method that further improves the performance of CS-MIMO radar in the colocated case. The method proceeds by minimizing the difference between the Gramian matrix of the sensing matrix and an identity matrix with respect to the vector of the transmitted waveforms, while the total transmitted power is fixed. Although the design is suboptimal, simulations have indicated substantial detection performance improvement as compared with the already good performance corresponding to the Hadamard waveform. The improvement is clearly observed at the very low PFA range, which is the only region in which the Hadamard waveform did not yield good performance.

## APPENDIX

It holds that

$$|\mathbf{u}_{k'}^H \mathbf{u}_k|^2 = u_{kk'} |\tilde{\mathbf{p}}^H \mathbf{B}_{kk'} \tilde{\mathbf{p}}|^2 = u_{kk'} \left[ (\tilde{\mathbf{p}}^H \mathbf{Br}_{kk'} \tilde{\mathbf{p}})^2 + (\tilde{\mathbf{p}}^H \mathbf{Bi}_{kk'} \tilde{\mathbf{p}})^2 \right] \tag{21}$$

where $u_{kk'} = \left| \sum_{l=1}^{N_r} e^{j2\pi \frac{(\eta_l^r(a_k) - \eta_l^r(a_{k'}))f}{c}} \right|^2$, $\mathbf{B}_{kk'} = \mathbf{V}^H(a_{k'}) \mathbf{X}^H \mathbf{\Phi}^H \mathbf{\Phi} X \mathbf{V}(a_k)$, $\mathbf{Br}_{kk'} = \frac{\mathbf{B}_{kk'} + \mathbf{B}_{kk'}^H}{2}$, and $\mathbf{Bi}_{kk'} = \frac{\mathbf{B}_{kk'} - \mathbf{B}_{kk'}^H}{2j}$. It is easy to see that $\mathbf{B}_{kk'}$ is not a positive semidefinite (PSD) matrix unless $k = k'$ and thus the objective function is nonconvex. However, we can make the objective function convex via the following trick:

$$\begin{aligned} (\tilde{\mathbf{p}}^T \mathbf{Br}_{kk'} \tilde{\mathbf{p}})^2 &= (\tilde{\mathbf{p}}^T (\underbrace{\mathbf{Br}_{kk'} + \frac{b}{P_t} \mathbf{I}}_{\mathbf{Cr}_{kk'}}) \tilde{\mathbf{p}} - b)^2 \\ &= (\tilde{\mathbf{p}}^T \mathbf{Cr}_{kk'} \tilde{\mathbf{p}})^2 + \tilde{\mathbf{p}}^T (-2b \mathbf{Cr}_{kk'} + \underbrace{\frac{d}{P_t} \mathbf{I}}_{\mathbf{Dr}_{kk'}}) \tilde{\mathbf{p}} + C_r \end{aligned} \tag{22}$$

where $b$ and $d$ are nonnegative real scalars that let $\mathbf{Cr}_{kk'}$ and $\mathbf{Dr}_{kk'}$ be PSD matrices, i.e., $\frac{b}{P_t} + \lambda_{\min}(\mathbf{Br}_{kk'}) \geq 0$ and $\frac{d}{P_t} + \lambda_{\min}(-2b\mathbf{Cr}_{kk'}) \geq 0$. $C_r$ is a constant that will not affect the objective function.

Equation (22) is convex since $\mathbf{Cr}_{kk'}$ and $\mathbf{Dr}_{kk'}$ are PSD matrices. By performing the same trick on $(\tilde{\mathbf{p}}^H \mathbf{Bi}_{kk'} \tilde{\mathbf{p}})^2$, we can obtain

$$(\tilde{\mathbf{p}}^T \mathbf{Bi}_{kk'} \tilde{\mathbf{p}})^2 = (\tilde{\mathbf{p}}^T \mathbf{Ci}_{kk'} \tilde{\mathbf{p}})^2 + \tilde{\mathbf{p}}^T (\mathbf{Di}_{kk'}) \tilde{\mathbf{p}} + C_i \tag{23}$$

In the same way, the second term in the objective function (13) can be rewritten as

$$\begin{aligned} |\mathbf{u}_k^H \mathbf{u}_k - P_t N_r|^2 &= N_r^2 (\tilde{\mathbf{p}}^T (\mathbf{B}_{kk} - \mathbf{I}) \tilde{\mathbf{p}})^2 \\ &= (\tilde{\mathbf{p}}^T \mathbf{C}_{kk} \tilde{\mathbf{p}})^2 + \tilde{\mathbf{p}}^T (\mathbf{D}_{kk}) \tilde{\mathbf{p}} + C \end{aligned} \tag{24}$$

Then the objective function of (13) can be transformed into a convex function as follows

$$\begin{aligned} &\min_{\tilde{\mathbf{p}}} \sum_{k \neq k'} (\tilde{\mathbf{p}}^T \mathbf{Cr}_{kk'} \tilde{\mathbf{p}})^2 + (\tilde{\mathbf{p}}^T \mathbf{Ci}_{kk'} \tilde{\mathbf{p}})^2 + \tilde{\mathbf{p}}^T (\mathbf{Dr}_{kk'} + \mathbf{Di}_{kk'}) \tilde{\mathbf{p}} \\ &\quad + \sum_k (\tilde{\mathbf{p}}^T \mathbf{C}_{kk} \tilde{\mathbf{p}})^2 + \tilde{\mathbf{p}}^T (\mathbf{D}_{kk}) \tilde{\mathbf{p}} \\ &\quad s.t.\ \tilde{\mathbf{p}}^H \tilde{\mathbf{p}} = P_t,\ \tilde{\mathbf{p}} \geq \mathbf{0}_{Mt \times 1}, \tilde{\mathbf{p}} \leq \sqrt{P_m} \mathbf{1}_{Mt \times 1} \end{aligned} \tag{25}$$

Looking at the constraints of (25), we can see that the first constraint is nonconvex. We can approximate that constraint by its local affine approximation, i.e.,

$$(\tilde{\mathbf{p}})^T \tilde{\mathbf{p}} \approx (\tilde{\mathbf{p}}^j)^T \tilde{\mathbf{p}}^j + 2(\tilde{\mathbf{p}}^j)^T (\tilde{\mathbf{p}} - \tilde{\mathbf{p}}^j) \tag{26}$$

where $(\tilde{\mathbf{p}}^j)$ is the estimate of $\tilde{\mathbf{p}}$ at the $j$-th iteration. The solution to (25) can be obtained in an iterative fashion as follows.

1) Set $\tilde{\mathbf{p}}^{(0)} = [1, 1, \ldots, 1]^T$ at the initial iteration.

2) At the $j$-th iteration, $\tilde{\mathbf{p}}^{(j)}$ is obtained by solving

$$\begin{aligned} &\min_{\tilde{\mathbf{p}}} \sum_{k \neq k'} \left| \mathbf{u}_{k'}^H \mathbf{u}_k \right|^2 + \sum_k \left| \mathbf{u}_k^H \mathbf{u}_k - P_t N_r \right|^2 \\ &s.t.\ (\tilde{\mathbf{p}}^{(j-1)})^H \tilde{\mathbf{p}}^{(j-1)} + 2(\tilde{\mathbf{p}}^{(j-1)})^H (\tilde{\mathbf{p}} - \tilde{\mathbf{p}}^{(j-1)}) \\ &\quad = P_t, \tilde{\mathbf{p}} \geq 0_{M_t \times 1}, \tilde{\mathbf{p}} \leq \sqrt{P_m} 1_{M_t \times 1} \end{aligned}$$

3) If the stop criterion is not satisfied, go to 2); otherwise, output $\tilde{\mathbf{p}} = \tilde{\mathbf{p}}^{(j)}$.

REFERENCES


[1] Haimovich, A. M., Blum, R. S., and Cimini, L. J.
MIMO radar with widely separated antennas.
*IEEE Signal Processing Magazine*, **25**, 1 (Jan. 2008), 116–129.

[2] Stoica, P., and Li, J.
MIMO radar with colocated antennas.
*IEEE Signal Processing Magazine*, **24**, 5 (2007), 106–114.

[3] Donoho, D. V.
Compressed sensing.
*IEEE Transactions on Information Theory*, **52**, 4 (Apr, 2006), 1289–1306.

[4] Candes, E. J., and Wakin, M. B.
An introduction to compressive sampling [A sensing/sampling paradigm that goes against the common knowledge in data acquisition].
*IEEE Signal Processing Magazine*, **25**, 2 (Mar. 2008), 21–30.

[5] Candes, E. J., Romberg, J. K., and Tao, T.
Stable signal recovery from incomplete and inaccurate measurements.
*Communications on Pure and Applied Mathematics*, **59**, 8 (Aug. 2006), 1207–1223.

[6] Candes, E. J., and Tao, T.
Near-optimal signal recovery from random projections: Universal encoding strategies?
*IEEE Transactions on Information Theory*, **52**, 12 (Dec. 2006), 5406–5425.

[7] Petropulu, A. P., Yu, Y., and Poor, H. V.
Distributed MIMO radar using compressive sampling.
In *Proceedings of 42nd Asilomar Conference on Signals, Systems and Computers*, Pacific Grove, CA, Nov. 2008, pp. 203–207.

[8] Chen, C., and Vaidyanathan, P. P.
MIMO radar space-time adaptive processing using prolate spheroidal wave functions.
*IEEE Transactions on Signal Processing*, **56**, 2 (Feb. 2008), 623–635.

[9] Yu, Y., Petropulu, A. P., and Poor, H. V.
MIMO radar using compressive sampling.
*IEEE Journal of Selected Topics in Signal Processing*, **4**, 1 (Feb. 2010), 146–163.

[10] Wang, S., He, Q., and He, Z.
Compressed sensing moving target detection for MIMO radar with widely spaced antennas.
In *Proceedings of 2010 International Symposium on Intelligent Signal Processing and Communication Systems* (ISPACS 2010), Cheng Du, China, Dec. 2010, pp. 1–4.

[11] Gogineni, S., and Nehorai, A.
Target estimation using sparse modeling for distributed MIMO radar.
*IEEE Transactions on Signal Processing*, **59**, 11 (Nov. 2011), 5315–5325.

[12] Yu, Y., Petropulu, A. P., and Huang, J.
Exploring sparsity in widely separated MIMO radar.
In *Proceedings of 45th Asilomar Conference on Signals, Systems and Computers*, Pacific Grove, CA, Nov. 2011.

[13] Yu, Y., Petropulu, A. P., and Poor, H. V.
CSSF MIMO Radar: Low-complexity compressive sensing based MIMO radar that uses step frequency.
*IEEE Transactions on Aerospace and Electronic Systems*, **48**, 2 (Apr. 2012), 1490–1504.

[14] Gurbuz, A. C., McClellan, J. H., and Scott, W. R.
A compressive sensing data acquisition and imaging method for stepped frequency GPRs.
*IEEE Transactions on Signal Processing*, **57**, 7 (July 2009), 2640–2650.

[15] Yoon, Y.-S., and Amin, M. G.
Imaging of behind the wall targets using wideband beamforming with compressive sensing.
In *Proceedings of IEEE Workshop on Statistical Signal Processing* (SSP2009), Cardiff, Wales, Aug. 2009, pp. 93–96.

[16] Yu, Y., Petropulu, A. P., and Poor, H. V.
The measurement matrix design for compressive sensing based MIMO radar.
*IEEE Transactions on Signal Processing*, **59**, 11 (Nov. 2011), 5338–5352.

[17] Yu, Y., and Petropulu, A. P.,
Power allocation for CS-based colocated MIMO radar systems.
*The Seventh IEEE Sensor Array and Multichannel Signal Processing Workshop* (SAM), Hoboken, NJ, June 2012.

[18] Godrich, H., Petropulu, A. P., and Poor, H. V.
Power allocation strategies for target localization in distributed multiple-radar architectures.

*IEEE Transactions on Signal Processing*, **59**, 7 (July 2011), 3226–3240.

[19] Akhtar, J.
Power allocation strategies for target localization in distributed multiple-radar architectures.
In *Proceedings of 11th International Radar Symposium*, Vilnius, Lithuania, June 2010, pp. 1–4.

[20] Chen, S. S., Donoho, D. L., and Saunders, M. A.
Atomic decomposition by basis pursuit.
*SIAM Journal on Scientific Computing*, **20**, 1 (1999), 33–61.

[21] Cai, T. T., and Wang, L.
Orthogonal matching pursuit for sparse signal recovery with noise.
*IEEE Transactions on Information Theory*, **57**, 7 (July 2011), 4680–4688.

[22] Efron, B., Hastie, T., Johnstone, I., and Tibshirani, R.
Least angle regression.
*Annals of Statistics*, **32**, 2 (2004), 407–499.

[23] Huang, J., and Zhang, T.
The benefit of group sparsity.
*Annals of Statistics*, **38**, 4 (2010), 1978–2004.

[24] Friedman, J., Hastie, T., and Tibshirani, R.
A note on the group lasso and a sparse group lasso. [Online].
*statweb.stanford.edu/tibs/ftp/sparse–grlasso.pdf*.

[25] Chen, X., Lin, Q., Kim, S., Carbonell, J. G., and Xing, E. P.
An efficient proximal gradient method for general structured sparse learning. [Online].
*arxiv.org/PS_cache/arxiv/pdf*/1005/1005.4717v3, 2010.

[26] Combettes, P. L., and Pesquet, J.-C.
Proximal splitting methods in signal processing. [Online].
*arxiv.org/abs*/0912.3522v4, 2010.

[27] Nocedal, J., and Wright, S. J.
*Numerical Optimization*. New York: Springer, 2006.

[28] Candes, E., and Tao, T.
The Dantzig selector: Statistical estimation when $p$ is much larger than $n$.
*Annals of Statististics*, **35** (2007), 2313–2351.

[29] Grant, M., and Boyd, S.
CVX: Matlab software for disciplined convex programming, version 2.0 beta. [Online]. http://cvxr.com/cvx, Sept. 2013. Accessed March 2013.

**Yao Yu** received the B.S. degree in the Telecommunication Engineering from Xidian University, Xian, China, in 2005, and the Mphil. degree from City University of Hong Kong, Hong Kong, in 2007. She received her Ph.D. degree in the Electrical Engineering from Drexel University, Philadelphia, in 2010. She was a postdoctoral assocate and visiting scholar at Rutgers, The State University of New Jersey from 2011 to 2013. Her research interests currently include signal processing on wireless communications and MIMO radar systems.

**Shunqiao Sun** received the B.E. degree in Electrical Information Engineering from Southern Yangtze University, Wuxi, China, in 2004, the M.S. degree in Communication and Information Systems from Fudan University, Shanghai, China, in 2011. From July 2004 to August 2008, he worked for Kinpo Electronics as a hardware engineer, focusing on embedded systems design. Since September 2011, he has been working towards the Ph.D. degree at the Department of Electrical & Computer Engineering, Rutgers University, New Brunswick, NJ, where he is a member of the Signal Processing and Communications Laboratory (CSPL). His research interests are in the area of wireless communications and radar systems, including cognitive radio networks, compressive sensing and matrix completion based MIMO radar.

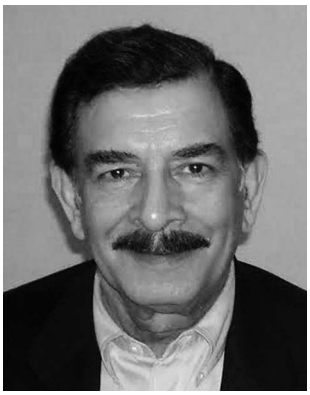

**Dr. Rabinder N. Madan** is a Life Fellow of the IEEE and a Fellow of the Institute of Mathematics and its Applications. He received his B.Sc. (Hons) and M.Sc. in Physics from St. Stephen's College, Delhi and a Ph. D. in Theoretical Physics from Princeton University. Currently he is a Chief Scientist at Champana Scientific, LLC. His interests and publications are in information sciences, signal processing, communications theory, nonlinear phenomenon, variation and optimization principles and scattering theory. As Program Manager of Systems Theory (1984–2012) at ONR he directed and managed programs in Statistical Signal Processing, Information Data Fusion and Communications. In the prior years he held faculty and Visiting Scholar positions at the Universities of California, Massachusetts, North Carolina and George Washington Universities and was a Senior Scientist at Hughes. In 1989 he was awarded the IETE J. C. Bose Memorial Award for the best paper in Science and Engineering. In 2010 he received the Best Paper Award in Cognitive Sensor Fusion at the IEEE 2010 MFI Conference. He is the recipient of the IEEE 2010 Harry Diamond Award for technical achievements. He served as the Editor-in- Chief of the Journal of the Franklin Institute (1993–2010) and is credited with having initiated the era of Special Issues and papers having a long shelf life.

**Athina P. Petropulu** received her undergraduate degree from the National Technical University of Athens, Greece, and the M.Sc. and Ph.D. degrees from Northeastern University, Boston MA, all in Electrical and Computer Engineering. Between 1992–2010 she was faculty at the Department of Electrical and Computer Engineering at Drexel University. Since 2010, she is Professor and Chair of the Electrical and Computer Engineering Department at Rutgers, The State University of New Jersey. She has held visiting appointments at SUPELEC in France and at Princeton University. Dr. Petropulu's research interests span the area of statistical signal processing with applications in wireless communications, networking and radar systems. She is recipient of the 1995 Presidential Faculty Fellow Award in Electrical Engineering given by NSF and the White House. She is the co-author (with C.L. Nikias) of the textbook entitled, "Higher-Order Spectra Analysis: A Nonlinear Signal Processing Framework," (Englewood Cliffs, NJ: Prentice-Hall, Inc., 1993).

Dr. Petropulu is Fellow of IEEE. She has served as Editor-in-Chief of the IEEE Transactions on Signal Processing (2009–2011), IEEE Signal Processing Society Vice President-Conferences (2006–2008), and member-at-large of the IEEE Signal Processing Board of Governors. She was the General Chair of the 2005 International Conference on Acoustics Speech and Signal Processing (ICASSP-05), Philadelphia PA. She is co-recipient of the 2005 IEEE Signal Processing Magazine Best Paper Award, and the 2012 Meritorious Service Award from the IEEE Signal Processing Society.